First observation of $H^{15}NO_3$ in atmospheric spectra

G. Brizzi,[1] M. Carlotti,[1] J.-M. Flaud,[2] A. Perrin,[2] and M. Ridolfi[1]

Received 6 October 2006; revised 6 December 2006; accepted 14 December 2006; published XX Month 2007.

[1] Using new and accurate experimental results concerning the spectroscopic properties of the $H^{14}NO_3$ and $H^{15}NO_3$ molecules, as well as improved theoretical methods, it has been possible to generate an improved set of line parameters for these molecules in the 11.2 μm spectral region. These line parameters were used to detect for the first time the $H^{15}NO_3$ molecule in the atmosphere analyzing atmospheric spectra recorded by the MIPAS (Michelson Interferometer for Passive Atmospheric Sounding) experiment. The evidence of $H^{15}NO_3$ in the atmosphere was achieved exploiting the features of the Residual and Error Correlation analysis. **Citation:** Brizzi, G., M. Carlotti, J.-M. Flaud, A. Perrin, and M. Ridolfi (2007), First observation of $H^{15}NO_3$ in atmospheric spectra, *Geophys. Res. Lett.*, *34*, LXXXXX, doi:10.1029/2006GL028395.

1. Introduction

[2] Because of its atmospheric interest, the HNO_3 molecule has been the subject of a number of spectroscopic studies, particularly in the 11.2 μm spectral region [see *Flaud et al.*, 2003, 2006, and references therein; *Perrin et al.*, 2004; *Mencaraglia et al.*, 2006] which is, as an atmospheric window, widely used for the atmospheric retrievals [*Ridolfi et al.*, 2000] of ^{14}N nitric acid. However, only recently accurate spectral line parameters were generated for the isotopic species $H^{15}NO_3$ [*Perrin and Mbiaké*, 2006]. Exploiting the high signal-to-noise ratio attained by the Michelson Interferometer for Passive Atmospheric Sounding (MIPAS) [*Fischer et al.*, 2000], we have investigated the possibility to detect for the first time $H^{15}NO_3$ in the atmosphere by analyzing its spectral signatures in the MIPAS atmospheric spectra. This is a first step toward the search for a possible enrichment of this molecule (with respect to the main isotopologue) in the stratosphere since stratospheric N_2O is known to be enriched isotopically relatively to tropospheric N_2O, most likely due to the preferential photolysis of isotopically light N_2O and to kinetic isotope effects [*Kaiser et al.*, 2002, 2006].

2. Spectroscopic Line Parameters

[3] In the 11.2 μm spectral region the HNO_3 absorption is mainly due to the fundamental ν_5 and the overtone $2\nu_9$ bands which are in strong interaction. Accordingly, the line positions and intensities of both $H^{14}NO_3$ and $H^{15}NO_3$ were generated using a Hamiltonian model and an intensity model which take fully into account the various vibro-rotational resonances as well as the torsional effects and the axis switching effect which have an impact on the spectra. In both cases, in order to get accurate Hamiltonian and transition moment constants, new analyses were performed by mixing the existing microwave data and series of high resolution Fourier transform infrared spectra (^{15}N enriched for $H^{15}NO_3$). Then using these constants new line lists of positions and intensities have been generated allowing one to better model the HNO_3 spectra [*Perrin et al.*, 2004; *Perrin and Mbiaké*, 2006]. It is worth noticing that, if the bands of both isotopic species are subject to the same interactions (strong Fermi and weaker Coriolis resonances), the mixing coefficients of the wave functions resulting from the diagonalization of the Hamiltonian matrices are widely different from one isotopologue to the other. As a consequence, the transfers of intensity from the fundamental band to the overtone are widely different in the two isotopologues. More precisely, whereas the $2\nu_9$ and ν_5 bands of $H^{14}NO_3$ have an intensity ratio of about 0.75 this ratio is about 0.22 for $H^{15}NO_3$. This means that, on a relative basis, the ν_5 band of $H^{15}NO_3$ is much stronger than the ν_5 band of $H^{14}NO_3$. This can be seen in Figure 1 where we have plotted both simulated spectra. In particular the Q-branch of the ν_5 band of $H^{15}NO_3$ is much stronger than the corresponding Q-branch of $H^{14}NO_3$. This favorable situation pushed us to search for the evidence of the ν_5 spectral signature of $H^{15}NO_3$ in atmospheric limb-emission spectra measured by MIPAS.

3. Observation of the Q-Branch of the ν_5 Band of $H^{15}NO_3$ in the MIPAS Spectra

[4] The Michelson Interferometer for Passive Atmospheric Sounding, onboard of the ENVISAT satellite, measures the atmospheric limb-emission spectrum in the middle-infrared. From July 2002 to March 2004 MIPAS has been measuring with an unapodized spectral resolution of 0.035 cm^{-1} Full Width at Half Maximum (FWHM). In this period MIPAS observations were acquired mainly in the so called "nominal mode", consisting of along-track, backward looking, limb-scans in the altitude range from 6 to 68 km, with tangent altitude increments of 3 km in the range from 6 to 42 km and coarser steps above.

[5] As a working hypothesis for the identification of $H^{15}NO_3$ in the MIPAS observations we have assumed, for this molecule, an altitude distribution equal to the one of the main isotopologue (determined from the same MIPAS measurements) multiplied by the factor of 0.00365 that corresponds to the $^{15}N/^{14}N$ natural isotopic ratio. With this assumption, the simulated MIPAS radiances show that the maximum intensity of the ν_5 Q-branch slightly exceeds 20 nW/(cm^2 sr cm^{-1}) in apodized spectra and occurs for tangent altitudes around 20 km at about 871 cm^{-1}. At this

[1]Dipartimento di Chimica Fisica e Inorganica, Università di Bologna, Bologna, Italy.
[2]Laboratoire Interuniversitaire des Systèmes Atmosphériques, CNRS, Universités Paris XII and VII, Créteil, France.

0094-8276/07/2006GL028395$05.00

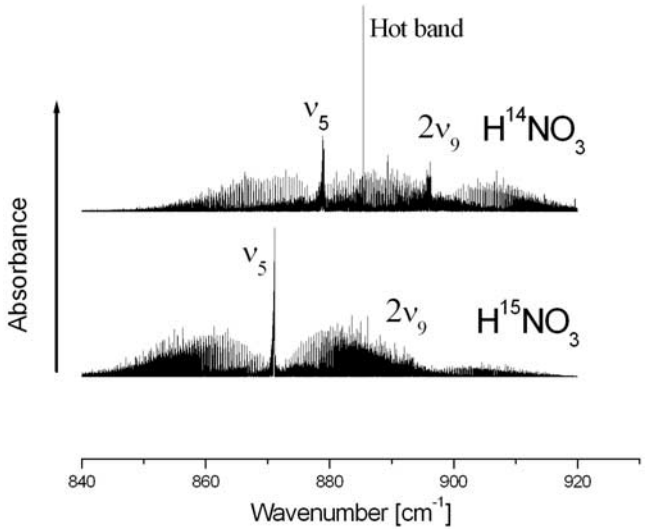

Figure 1. $H^{14}NO_3$ and $H^{15}NO_3$ simulated spectra. The intensity ratios of the ν_5 and $2\nu_9$ bands are very different for the two isotopic species. In particular note the strong intensity of the Q-branch of the ν_5 band of $H^{15}NO_3$ (see text).

frequency the apodized Noise Equivalent Spectral Radiance (NESR) is also about 20 nW/(cm^2 sr cm^{-1}) in the observed MIPAS spectra; these numbers require then to search for the $H^{15}NO_3$ signature on averages of spectra in order to reduce the NESR to a level significantly smaller than the signal of the ν_5 Q-branch. For this purpose we have selected good-quality and probably cloud-free [*Remedios et al.*, 2003] observations acquired during the well-characterized and consolidated ENVISAT orbit 2081 (from 24 July 2002). Two sets of 213 spectra each were averaged within the tangent altitude ranges from 15 to 23 km, and from 24 to 32 km and apodized as outlined below. The NESR affecting the average apodized spectra is then expected to be 1.5 nW/(cm^2 sr cm^{-1}).

[6] The strategy devised for the detection of $H^{15}NO_3$ in the atmosphere consists in the comparison of the average apodized MIPAS spectra with the corresponding average of apodized synthetic spectra. Synthetic spectra were calculated both with (simulations of type A) and without (simulations of type B) the contribution of the ν_5 Q-branch transitions of $H^{15}NO_3$. The individual synthetic spectra were generated using the MIPAS Level-2 products retrieved by the ground processor of the European Space Agency (ESA) by analyzing the same set of measured spectra; furthermore, the chemical species not retrieved by ESA were assumed to be distributed according to their climatological average [*Remedios*, 1999] relating to season and latitude band of the corresponding observation. The forward model used to generate the synthetic spectra includes the capability of modeling the horizontal variability of the atmosphere and was derived from the algorithm described in the work of *Carlotti et al.* [2006]. Figure 2 refers to the 15–23 km tangent altitudes range, and a frequency interval where the ν_5 Q-branch of $H^{15}NO_3$ is expected to appear. Figure 2a shows the average measured spectrum (solid line) and the average simulation of type A (dashed line); the evident spectral features in Figure 2a are due to the main isotopologue of nitric acid. The solid line Figure 2b shows the residual spectrum (solid minus dashed lines of Figure 2a). From Figure 2 it is clear that there is a significant discrepancy between average observation and simulation, due to a background signal, making tricky the visual interpretation of the residual. In the 24–32 km tangent altitudes range the size of the discrepancy due to the background signal is about half the one in Figure 2.

[7] In order to provide a reliable interpretation of the residuals we decided to exploit the Residual and Error Correlation (REC) analysis [*Dudhia*, 2002; *Flaud et al.*, 2006] that permits to characterize objectively a residual spectrum in terms of its consistency with the known error sources that may affect both the observed and the simulated spectra. The REC analysis was applied to the simulations obtained with the contribution of the $H^{15}NO_3$ transitions (type A simulations) and considering all the known error sources due to both the instrument and the atmospheric models but the errors due to the HNO_3 distribution and to the spectroscopic data. The REC analysis highlighted that it is possible to capture the shape of the observed residual spectrum using a linear combination of known error contributions. Among these, the dominating contributions are the instrumental offset and any error source that acts as an atmospheric continuum, i.e. with a frequency-independent

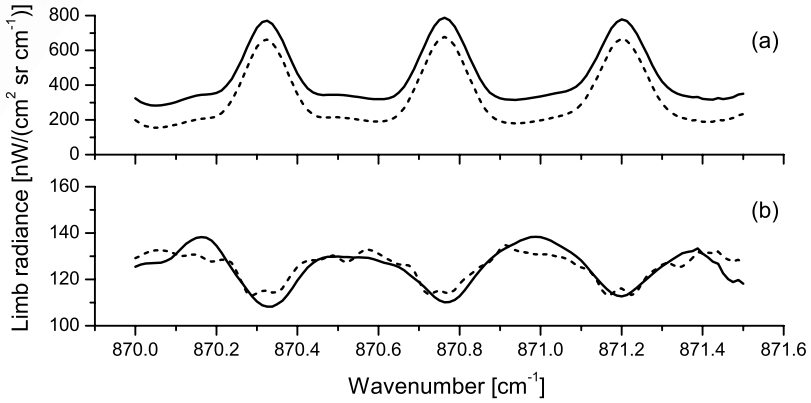

Figure 2. (a) Average of 213 MIPAS apodized spectra in the 15–23 km tangent altitude range (solid line) and the corresponding simulation that includes the $H^{15}NO_3$ transitions (dashed line). (b) Residual spectrum (solid line: solid minus dashed lines of Figure 2a) and the residual spectrum simulated by the REC analysis (dashed line).

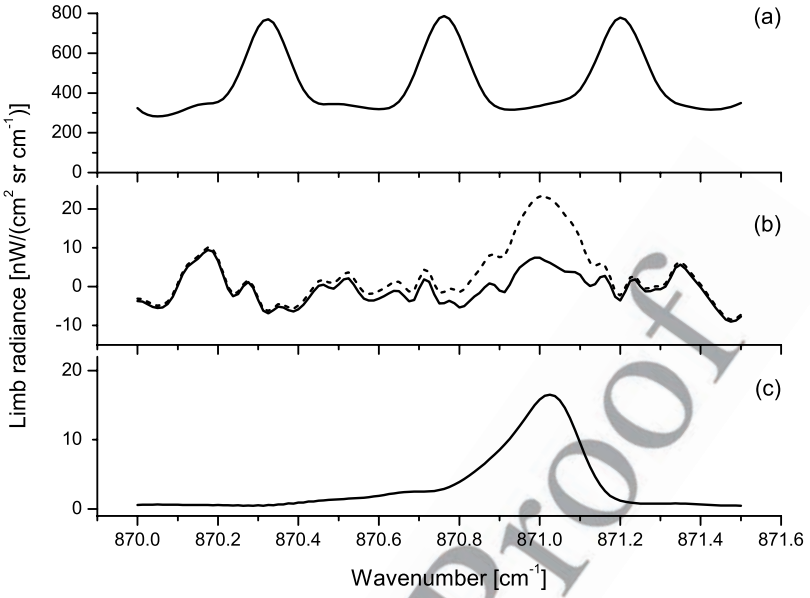

Figure 3. (a) Average of 213 MIPAS spectra in the 15–23 km tangent altitude range. (b) Difference between the spectrum in Figure 3a and the corresponding simulation that includes the $H^{15}NO_3$ transitions (solid line) and the difference between the spectrum in Figure 3a and the simulation without the $H^{15}NO_3$ transitions (dashed line). (c) Difference between simulated spectra including and excluding $H^{15}NO_3$, i.e. difference between the dashed and continuous lines in Figure 3b.

contribution to the absorption coefficient. Figure 2b illustrates how the REC-analysis simulated residual (dashed line) fits the observed average residual (solid line) in the altitude range from 15 to 23 km.

[8] Our forward model considers for the simulation all the transitions included in the HITRAN_MIPAS_PF_3.2 database [*Flaud et al.*, 2006] up to 25 cm^{-1} away from each spectral element, furthermore it includes the models for the main gaseous continua (H_2O, N_2, O_2) [*Clough*, 1995; *Lafferty et al.*, 1996; *Thibault et al.*, 1997]. Therefore we think that such a large continuum-like discrepancy detected in the residuals could be attributed to one or several of the following causes:

[9] 1. Inaccuracy of the adopted models for gaseous continua. However this is a pretty unlikely hypothesis as in the considered altitude range the contribution of gaseous continua is negligible compared to the measurement noise.

[10] 2. Underestimated amount of CFC12 in the simulations. This CFC contributes to the limb radiance observed in the considered spectral region, however this hypothesis is also unlikely since the concentration of CFC12 is relatively well known.

[11] 3. Possible presence in the field of view of some limb-observations of high clouds (around the equator) and PSCs (over the Antarctic polar winter) that are not accounted for in our forward model.

[12] Among these causes, contamination of observations by clouds is considered the most likely due to the amplitude of the produced error on the residuals.

[13] Regarding the instrumental offset detected by the REC analysis, since its effect on the spectrum is very similar to the effect of any continuum-like contribution, it is measured with a very large error. Despite of that, the instrumental offset obtained from the REC analysis is consistent with the specified MIPAS radiometric accuracy.

[14] The simulated residual spectrum best fitting the one observed with simulations of type A was then added to the average simulations of both types A and B in order to compensate for the errors identified by the REC analysis. After this correction, the average simulated spectra were again compared with the corresponding average observations. Figures 3 and 4 show the results of the comparison for the tangent altitude ranges from 15 to 23 km and from 24 to 32 km respectively. Figures 3a and 4a show the average observations. Figures 3b and 4b show the difference between the spectrum in Figures 3a and 4a and the corresponding REC analysis corrected simulation with (solid line) and without (dashed line) the $H^{15}NO_3$ transitions. Figures 3c and 4c show the difference between the dashed and the continuous lines of Figures 3b and 4b; the curves in Figures 3c and 4c represent the signal due to the $H^{15}NO_3$ transitions.

[15] All the observed and simulated spectra presented in this paper were apodized in order to attenuate the composite contribution of the sidelobes due to the strong spectral features of the HNO_3 main isotopologue. The adopted apodizing function is a modified "Norton-Beer strong" function [*Norton and Beer*, 1977] whose FWHM is 0.12 cm^{-1} that is narrower than the approximate FWHM of the ν_5 Q-branch which is about 0.22 cm^{-1}. This apodizing function is therefore suitable to damp the sidelobes without introducing a significant broadening the $H^{15}NO_3$ Q-branch.

[16] In Figures 3 and 4 the spectral contribution of $H^{15}NO_3$ is clearly visible and its variation with altitude is consistent with the assumed profile shape.

4. Conclusions

[17] Using the most recent and accurate spectral line parameters concerning $H^{14}NO_3$ and $H^{15}NO_3$ in the 11.2 μm

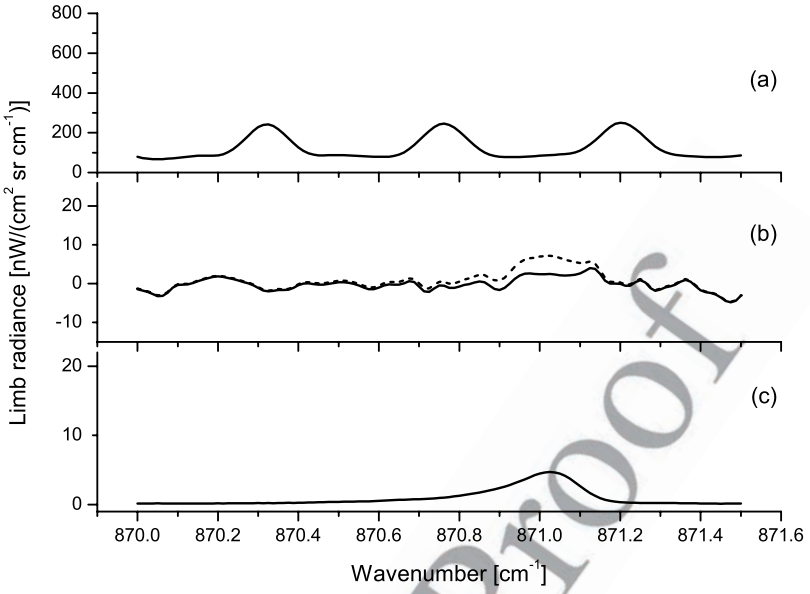

Figure 4. Same as Figure 3 but relative to the tangent altitude range from 24 to 32 km.

spectral region it has been possible to model accurately MIPAS spectra allowing to detect for the first time the spectral signature of $H^{15}NO_3$ in atmospheric spectra. A rough estimate, obtained comparing the intensity of the observed signals with the noise level, leads to estimate that the natural $^{15}N/^{14}N$ isotopic ratio of 0.00365 is observed with about 20% uncertainty in the stratospheric nitric acid. Further investigations are in progress in order to determine the altitude distribution of $H^{15}NO_3$ and verify, with a better accuracy, its possible enrichment in the stratosphere with respect to the natural ^{15}N isotopic abundance.

[18] **Acknowledgment.** The authors are grateful to Anu Dudhia from Oxford University for providing the error spectra used in this study.

References

Carlotti, M., G. Brizzi, E. Papandrea, M. Prevedelli, M. Ridolfi, B. M. Dinelli, and L. Magnani (2006), GMTR: Two-dimensional multi-target retrieval model for MIPAS/ENVISAT observations, *Appl. Opt.*, *45*, 716–727.

Clough, S. A. (1995), The water vapor continuum and its role in remote sensing, in *Optical Remote Sensing of the Atmosphere*, *Opt. Soc. of Am. Tech. Dig. Ser.*, vol. 2, pp. 76–78, Opt. Soc. of Am., Washington, D. C.

Dudhia, A. (2002), REC analysis of MIPAS data, *Eur. Space Agency Tech. Note*, *ESA PO-TN-OXF-GS-0020*.

Fischer, H., et al. (2000), Envisat-MIPAS: An instrument for atmospheric chemistry and climate research, *ESA Spec. Publ.*, *SP-1229*, 124 pp.

Flaud, J.-M., C. Piccolo, B. Carli, A. Perrin, L. H. Coudert, J.-L. Teffo, and L. R. Brown (2003), Molecular line parameters for the MIPAS (Michelson Interferometer for Passive Atmospheric Sounding) experiment, *Atmos. Oceanic Opt.*, *16*, 172–182.

Flaud, J.-M., G. Brizzi, M. Carlotti, A. Perrin, and M. Ridolfi (2006), MIPAS database: Validation of HNO_3 line parameters using MIPAS satellite measurements, *Atmos. Chem. Phys.*, *6*, 5037–5048.

Kaiser, J., C. A. M. Brenninkmeijer, and T. Röckmann (2002), Intramolecular ^{15}N and ^{18}O fractionation in the reaction of N_2O with $O(^1D)$ and its implications for the stratospheric N_2O isotope signature, *J. Geophys. Res.*, *107*(D14), 4214, doi:10.1029/2001JD001506.

Kaiser, J., A. Engel, R. Borchers, and T. Röckmann (2006), Probing stratospheric transport and chemistry with new balloon and aircraft observations of the meridional and vertical N_2O isotope distribution, *Atmos. Chem. Phys. Discuss.*, *6*, 4273–4324.

Lafferty, W. J., A. M. Solodov, A. Weber, W. B. Olson, and J.-M. Hartmann (1996), Infrared collision-induced absorption by N_2 near 4.3 μm for atmospheric applications: Measurements and empirical modelling, *Appl. Opt.*, *35*, 5911–5917.

Mencaraglia, F., G. Bianchini, A. Boscaleri, B. Carli, S. Ceccherini, P. Raspollini, A. Perrin, and J.-M. Flaud (2006), Validation of MIPAS satellite measurements of HNO_3 using comparison of rotational and vibrational spectroscopy, *J. Geophys. Res.*, *111*, D19305, doi:10.1029/2005JD006099.

Norton, R. H., and R. Beer (1977), New apodizing functions for Fourier spectrometry, *J. Opt. Soc. Am.*, *66*, 259–264. (Correction, *J. Opt. Soc. Am., 67*, 419, 1977.)

Perrin, A., and R. Mbiaké (2006), The ν_5 and $2\nu_9$ bands of the ^{15}N isotopic species of nitric acid ($H^{15}NO_3$): Line positions and intensities, *J. Mol. Spectrosc.*, *237*, 27–35.

Perrin, A., J. Orphal, J.-M. Flaud, S. Klee, G. Mellau, H. Mäder, D. Walbrodt, and M. Winnewisser (2004), New analysis of the ν_5 and $2\nu_9$ bands of HNO_3 by infrared and millimeter wave techniques: line positions and intensities, *J. Mol. Spectrosc.*, *228*, 375–391.

Remedios, J. J. (1999), Extreme atmospheric constituent profiles for MIPAS, paper presented at European Symposium on Atmospheric Measurements from Space, Eur. Space Res. and Technol. Cent., Eur. Space Agency, Noordwijk, Netherlands.

Remedios, J. J., R. Spang, and M. Ridolfi (2003), Detection of cloud effects in MIPAS observations and implementation in the operational processor, *Eur. Space Agency Tech. Rep.*, *ESA PO-TN-ULE-GS-0002*.

Ridolfi, M., et al. (2000), Optimized forward model and retrieval scheme for MIPAS near-real-time data processing, *Appl. Opt.*, *39*, 1323–1340.

Thibault, F., V. Menoux, R. Le Doucen, L. Rosenmann, J.-M. Hartmann, and C. Boulet (1997), Infrared collision-induced absorption by O_2 near 6.4 μm for atmospheric applications: Measurements and empirical modelling, *Appl. Opt.*, *36*, 563–567.

G. Brizzi, M. Carlotti, and M. Ridolfi, Dipartimento di Chimica Fisica e Inorganica, Università di Bologna, Viale del Risorgimento 4, I-40136 Bologna, Italia. (gabriele.brizzi@unibo.it)

J.-M. Flaud and A. Perrin, Laboratoire Interuniversitaire des Systèmes Atmosphériques, CNRS, Universités Paris XII and VII, 61 avenue du Général de Gaulle, F-94010 Créteil Cedex, France.